J Mater Sci (2011) 46:6830–6834
DOI 10.1007/s10853-011-5642-1

Growth of highly oriented iridium oxide bottom electrode for $Pb(Zr,Ti)O_3$ thin films using titanium oxide seed layer

L. Trupina · C. Miclea · L. Amarande · M. Cioangher

Received: 14 March 2011 / Accepted: 16 May 2011 / Published online: 1 June 2011

Abstract Due to its low resistivity and excellent thermal stability, IrO_2 has attracted attention as an alternative for electrode material in ferroelectric integrated circuit applications. Oriented growth of IrO_2 electrode film was investigated with the goal to control the texture of the PZT thin film. IrO_2 films were prepared by DC reactive sputtering. PZT film was prepared by RF magnetron sputtering single target deposition method. The whole layer stack was grown onto amorphous thermal oxide of a silicon wafer. The results indicate that IrO_2 thin film was preferentially (200) oriented when a TiO_2 seeding layer was used. The orientation relationships along the whole PZT(111)/IrO_2(200)/TiO_2(200)/Ti structure was discussed.

Introduction

There has been a great interest in ferroelectric thin films for integration with the IC technology, especially in connection with obtaining nonvolatile ferroelectric random access memory (NV-FRAM) devices. Lead-zirconate-titanate (PZT) thin film was the primary candidate for NV-FRAM applications since it has many advantages such as low processing temperature and high remanent polarization. As an alternative, $SrBi_2Ta_2O_9$ (SBT) thin film has received a great deal of attention because it has a lower coercive field, and excellent reliability properties as strong fatigue resistance and low imprint behavior. Although the physical properties of ferroelectric thin films have been extensively investigated, some aspects concerning the microstructure and growth of oriented $Pb(Zr_{1-x}Ti_x)O_3$ ferroelectric thin films, remained unclear. It is essential to study such phenomena to establish the right mechanisms governing orientation selection on different electrode layers. Because the ferroelectric properties of the PZT films originate in their structural anisotropy, it is essential to prepare highly textured thin films on highly textured bottom electrodes.

Bottom electrode has significant effects on the deposition characteristics, electrical properties, and device performances of PZT capacitors [1, 2]. The PZT capacitor with Pt electrode has good leakage current characteristics but suffers severe fatigue degradation [3], while the capacitor with RuO_2 electrode is fatigue-free but shows high leakage current density [4].

The control of bottom electrode orientation is the first step in obtaining oriented PZT thin films. Since the growth of PZT films is mainly controlled by nucleation, the electrode system must provide the necessary template function to obtain the required texture. In ferroelectric devices, a PZT layer with a (111) texture facilitates uniform polarization performance across various bits as ferroelectric capacitor sizes continue to shrink.

We studied the growth of oriented IrO_2 on TiO_2 seed layer, and its function to seed (111) oriented PZT. The most promising texture of IrO_2 layer seems to be the [100] crystal direction compared with the results obtained on (100)RuO_2 [5, 6]. The (111) preferentially oriented PZT thin films were obtained on (100)-oriented RuO_2 bottom electrode using metal–organic chemical vapor deposition method (MOCVD) [7] and reactive in situ sputtering. In both cases, the (100) orientation of the RuO_2 layer was obtained by using a Pt template layer, (111)-oriented on SiO_2/Si. These results clearly show that (111)-oriented polycrystalline PZT thin films can be grown on highly (100) oriented RuO_2 bottom electrode. In analogy with

L. Trupina (✉) · C. Miclea · L. Amarande · M. Cioangher
National Institute for Materials Physics, Magurele,
077125 Bucharest, Romania
e-mail: lucian.trupina@infim.ro

these results and due to their good electrical properties [8], we studied the controlled growth of oriented IrO_2 thin films, and its function to seed (111) oriented PZT without using the (111)Pt template.

Experimental setup

Experiments were carried out using an ULVAC SBR-1102E RF-sputtering single target system with target of 5 cm in diameter. A RF power supply with a 13.56 MHz frequency and maximum 600 W power was used to excite the plasma.

The films were deposited on SiO_2 layer formed by the *thermal oxidation* method of a Si wafer. Pre-sputtering of Ir and Ti targets was performed for 5 min at 100 and 200 W, respectively, before film's deposition. A 10-nm titanium thin film was deposited from a metallic target on a heated substrate at 600 °C, at 30 W applied power, and 12 mTorr Ar working pressure. A 3-nm TiO_2 thin film was deposited by reactive RF magnetron sputtering from a metallic Ti target at 10 mTorr O_2 working pressure and 650 °C substrate temperatures. A 200 nm, IrO_2 thin film was deposited by DC reactive sputtering at 600 °C substrate temperature and 10 mTorr O_2 working pressure.

The PZT thin films with a thickness of 200 nm were deposited onto $IrO_2/TiO_2/Ti$-coated SiO_2/Si wafers from a single PZT target at different substrate temperatures, working pressures, and applied powers. In all cases, PZT deposition was preceded by deposition of a 2 nm thick TiO_2 sacrificial barrier layer to prevent degradation of the IrO_2 surface and to allow better perovskite nucleation [9].

The formed structure is presented schematically in Fig. 1.

The preparation method of PZT target was the usual mixed oxide route. The details of this experimental procedure were already reported elsewhere [10].

The thickness of deposited layers was measured with a Dektak 3030 profilometer. The standard θ–2θ X-ray diffraction (XRD) Bruker equipment was used to study the film structure and orientation. The morphological analyses of the samples were carried out by means of a scanning electron microscope (SEM) (FEI Quanta Inspect F). Atomic force microscopy (AFM) (MFP 3D SA, Asylum Research) was used to obtain high-resolution images of the sample surface. The AFM used cantilevers with a spring constant of 2 N/m (Olympus AC240-TS) for imaging in AC mode. For ferroelectric measurements top electrodes (1×1 mm^2) consisted of IrO_2 were deposited by sputtering at room temperature through a mechanical mask. The dielectric properties of PZT thin films were measured with a HP4194A impedance analyzer. Polarization versus electric field hysteresis loops and fatigue of PZT thin film were recorded with a Precision II Radiant Technology system.

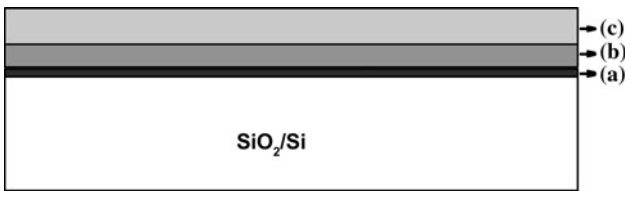

Fig. 1 PZT/$IrO_2/TiO_2/Ti/SiO_2/Si$ structure. (*a*) (3 nm) TiO_2/(10 nm) Ti seeding layers, (*b*) (200 nm) IrO_2 layer, and (*c*) (200 nm) PZT layer

Results and discussion

XRD patterns of IrO_2 thin films deposited on SiO_2/Si substrate at different working pressures (5, 10, and 15 mTorr) and different substrate temperatures (500, 600, and 700 °C) show only IrO_2 peaks which correspond to randomly oriented thin films. A few hours after deposition peeling of IrO_2 thin films is observed, regardless the deposition conditions. This fact was attributed to the intrinsic stress in IrO_2 thin films. Figure 2 shows the XRD pattern of unpeeled IrO_2 thin film deposited at 15 mTorr (Ar + O_2 50%) working gas pressure and 600 °C substrate temperature.

We have found that using an adhesion layer of TiO_2/Ti it is possible to grow adherent IrO_2 films with a preferred orientation.

Figure 3 shows the XRD pattern of 200 nm IrO_2 deposited on TiO_2/Ti where the IrO_2 thin film shows a (200) preferred orientation. We analyzed the intensity for the three maximum intensity lines (110), (200), and (221).

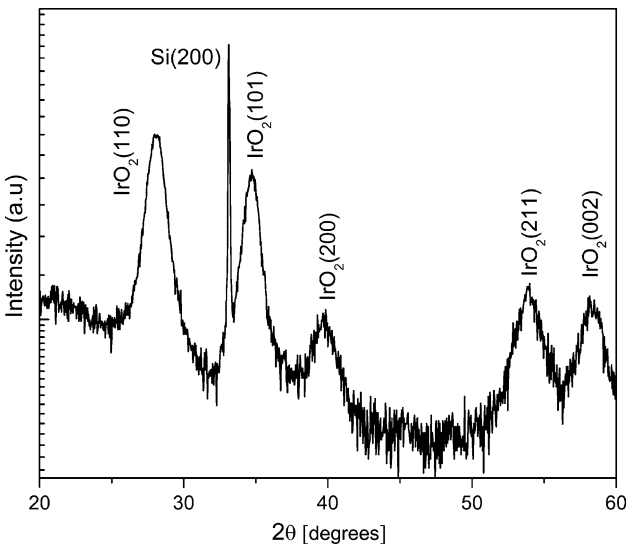

Fig. 2 XRD pattern of the as-grown random oriented IrO_2 film on SiO_2/Si at 15 mTorr, Ar + O_2 50%, 600 °C substrate temperature

According to PDF 43-1019, for a random iridium oxide powder mixture, the relative intensity for $I_{(110)}$, $I_{(200)}$, and $I_{(221)}$ are 100, 25, and 54, respectively. In order to determine the texture index for a given orientation, in our case the (200) orientation, we used the formula:

$$\alpha_{(200)} = \frac{\left(I_{(200)} \Big/ I^{*}_{(200)}\right)}{\sum \left(I_{(hkl)} \Big/ I^{*}_{(hkl)}\right)},$$

where I_{hkl} is the measured intensity of the (hkl) peak for the films, I^{*}_{hkl} is the relative intensity for powders. The calculated value for $\alpha_{(200)}$, representing the degree of (200) orientation, is 99%. The result suggests that the TiO_2 seeding layer has a decisive impact on the orientation of the IrO_2 thin films and the influence of the TiO_2 seed layer is more important than other process parameters such as substrate temperature during deposition, the working gas pressure or the power applied to the target.

The preferred (200) orientation of IrO_2 thin films may be explained in terms of the previously results obtained by Chen and co-workers [11].

They found that rutile TiO_2 films with (200) preferred orientation can be grown by thermal oxidation of sputtered Ti metal films. The highly crystalline Ti film with (002) orientation can induce the preferential growth of the resultant TiO_2 crystals with (200) orientation. In our case, the TiO_2 film was obtained by DC reactive sputtering and not by thermal oxidation. Figure 4 shows the XRD pattern of the TiO_2 thin film deposited on (3 nm) $Ti/SiO_2/Si$ substrate.

The most favorable matching occurs at the (200)TiO_2–(200)IrO_2 interface, for the atomic structures of (200) planes in rutile TiO_2 and (200) planes in rutile IrO_2, as it is schematically illustrated in Fig. 5.

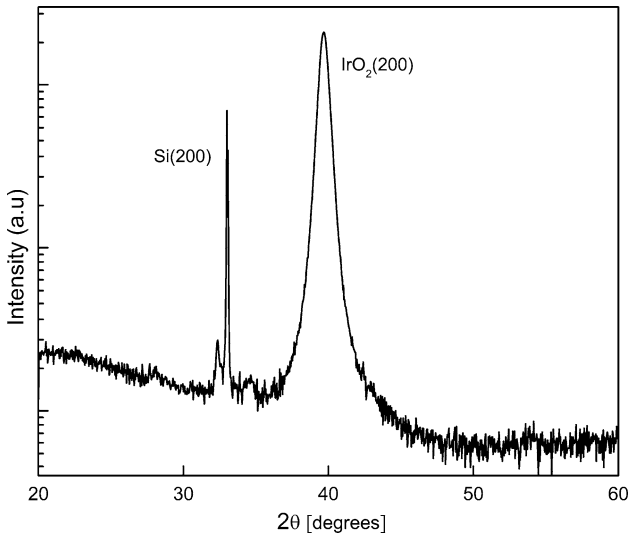

Fig. 3 XRD pattern of the as-grown (100)IrO_2 oriented film sputtered on $TiO_2/Ti/SiO_2/Si$

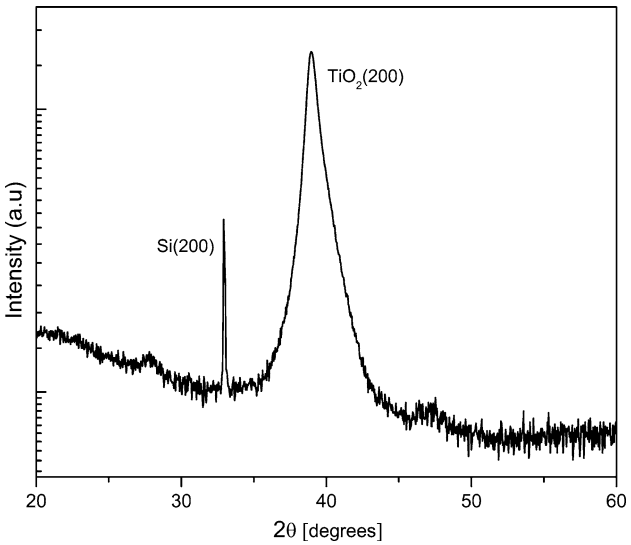

Fig. 4 XRD pattern of the as-grown TiO_2 film sputtered on $Ti/SiO_2/Si$

The lattice mismatch shown in Table 1 is relatively small: 2.1% for the b axis and 6.2% for the c axis.

Figure 6 shows the SEM image of the $IrO_2/TiO_2/Ti/SiO_2/Si$ thin film. The film is granular with an average grain size of about 80–100 nm. The surface morphology is smooth, free of cracks, and has an uniform grain size distribution indicating a well-defined microstructure.

The surface morphology of the IrO_2 thin films was also observed by AFM. The AFM measured rms roughness is 5.67 nm over a 27.7 μm^2 area (Fig. 7).

Sheet resistance was measured for IrO_2 thin films deposited at substrate temperature of 500 and 700 °C. The electrical resistivity decreases from 83 to 66 μΩ cm with increasing substrate temperature during deposition, being comparable with the electrical resistivity of 48 μΩ cm of IrO_2 single crystal [12, 13]. It is obvious that the IrO_2 thin film has a dense microstructure which is improved at higher substrate temperature deposition.

The crystalline structure of the PZT thin films was investigated using XRD method. Figure 8 shows an XRD

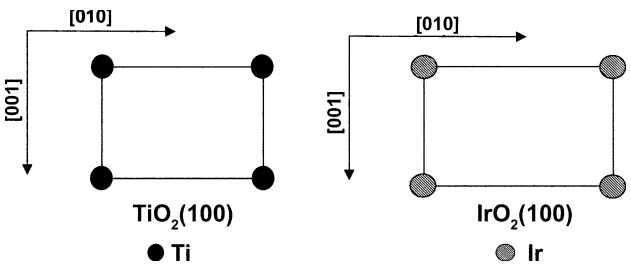

Fig. 5 Atomic structures of (100)TiO_2 and (100)IrO_2 planes

Table 1 Calculated in plane distances and lattice mismatches with $IrO_2(200)$ for $TiO_2(200)$ and $TiO_2(110)$

	Plane	Direction 1	Direction 2	d_1 (Å)	d_2 (Å)	Δ_1 (%)	Δ_2 (%)
IrO_2	(100)	[001]	[010]	3.154	4.498	0.0	0.0
TiO_2	(100)	[001]	[010]	2.959	4.593	−6.2	2.1
TiO_2	(110)	[001]	[−110]	6.496	2.959	205.1	34.2

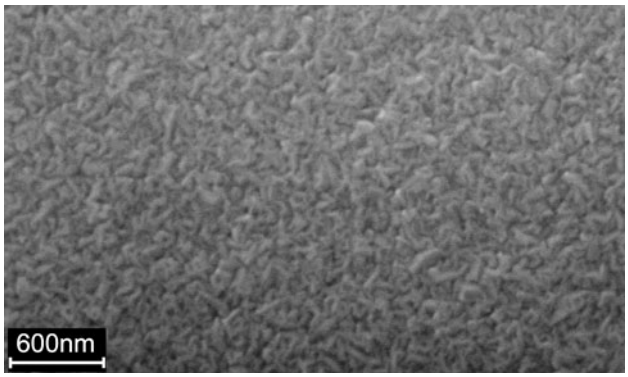

Fig. 6 SEM image of the $IrO_2/TiO_2/Ti/SiO_2/Si$ thin film

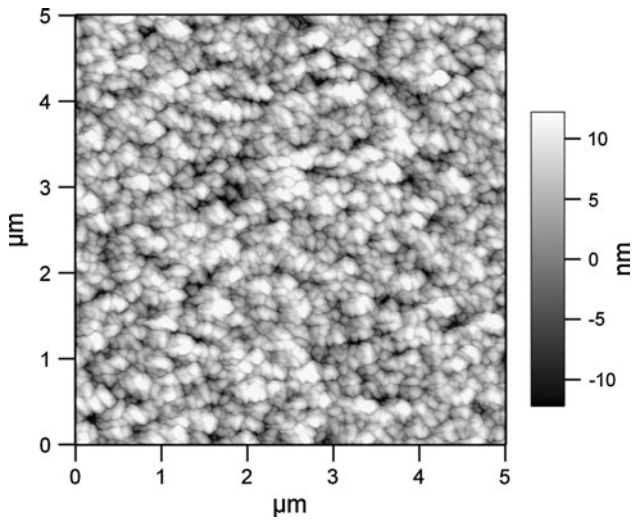

Fig. 7 AFM image of $IrO_2/TiO_2/Ti/SiO_2/Si$ thin film

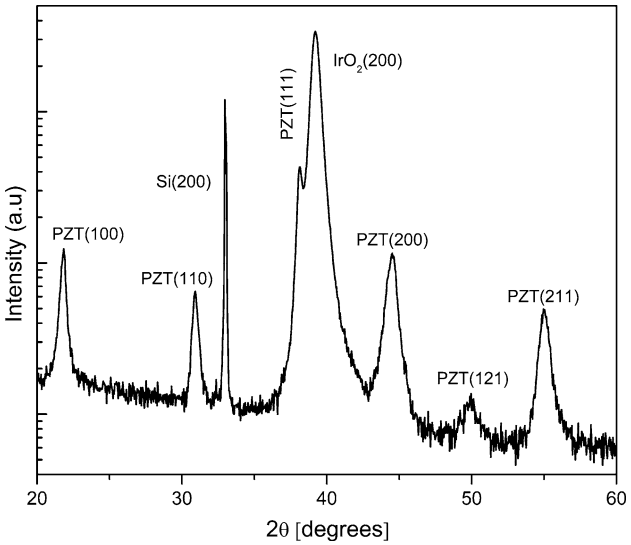

Fig. 8 XRD patterns of the (111)-oriented PZT deposited on $(200)IrO_2/TiO_2/Ti/SiO_2/Si$

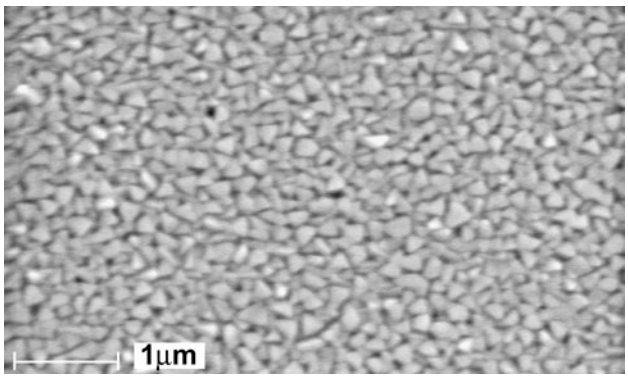

Fig. 9 SEM of as-deposited PZT thin film on $IrO_2/TiO_2/Ti/SiO_2/Si$ substrate

pattern of the PZT film deposited on the IrO_2/TiO_2/Ti-coated SiO_2/Si wafers. The XRD pattern reveals the pure perovskite structure with (111) preferential growth. The textured degree along the (111) direction is $\alpha_{(111)} = 86\%$. It also proves the correlation between the orientations of PZT(111) and $IrO_2(100)$ which is in agreement with the results of Maeder et al. [5] obtained on a similar system PZT/RuO_2

The surface morphology of the deposited PZT films was investigated by SEM. Figure 9 shows a SEM image of a top view of the PZT films deposited on the IrO_2/TiO_2/Ti-coated SiO_2/Si wafers. As shown in the SEM image, the deposited PZT film was dense, crack-free with a homogeneous microstructure, and grain size within the range of 150 nm to about 200 nm.

Both the phase structure (Fig. 8) and the very good microstructural characteristics (Fig. 9) indicate that the perovskite phase formation is completed during the PZT deposition and the deposited films are 86% textured along the (111) direction.

The hysteresis loops and the fatigue properties of the PZT thin film were measured. The P–E hysteresis loops measured, before and after 10^8 switching cycles, at a

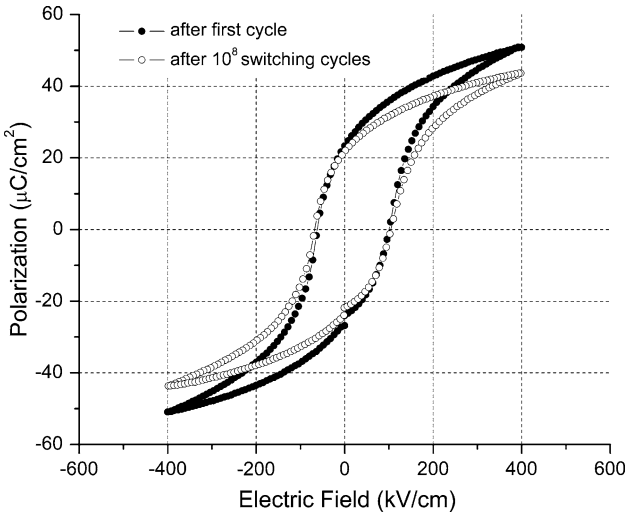

Fig. 10 The measured P–E hysteresis loops for $IrO_2/PZT/IrO_2$ capacitor before and after switching over 10^8 cycles

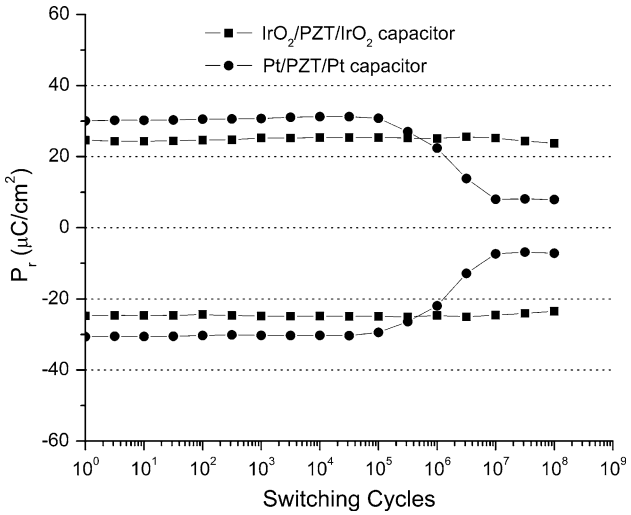

Fig. 11 Fatigue properties of Pt/PZT/Pt and $IrO_2/PZT/IrO_2$ capacitors

frequency of 10 kHz are shown in Fig. 10. The values for remanent polarization and the coercive field, *obtained from the virgin hysteresis* loop, are 22 μC/cm^2 and 100 kV/cm, respectively. Dielectric properties of $IrO_2/PZT/IrO_2$ capacitor were measured at 100 kHz frequency at room temperature using a HP4194A impedance analyzer. The typical values of dielectric constant and loss of the thin film are 700 and 0.03, respectively. The leakage current densities at a field of 100 and 150 kV were 4×10^{-4} and 1×10^{-4} A/cm^2, respectively.

Figure 11 presents the fatigue characteristics of the Pt/PZT/Pt and $IrO_2/PZT/IrO_2$ capacitors. It has been found that the single metal electrode layer usually exhibits a fatigue problem caused by oxygen vacancies, and thus oxide electrodes have been introduced to overcome this problem [14, 15].

It is shown that $2P_r$ values of the film deposited on Pt electrode start decreasing after 10^5 cycles down to 25% from initial value. The capacitor fabricated on IrO_2 electrode has negligible fatigue loss of around 3% after 10^8 switching cycles because the electrode acts as a sink for oxygen vacancies and lowers the concentration of the holes in PZT films.

Conclusions

The obtained results demonstrate the presence of a correlated orientation along the trilayer PZT(111)/IrO_2(200)/TiO_2(200) structure. The TiO_2 seeding layer has a decisive effect on the orientation of the IrO_2 thin films. The influence of the TiO_2 seed layer is more important than other processing parameters as substrate temperature and the working gas pressure. A 200 nm PZT thin films with highly oriented (111) perovskite phase were successfully grown at 600 °C on IrO_2(200)/TiO_2(200)/Ti structure by in situ RF magnetron sputtering. It is obvious that the IrO_2(200)/TiO_2(200)/Ti/SiO_2/Si structure allows the control of the PZT texture. The capacitors fabricated on IrO_2 electrode showed high values of the initial $2P_r$ and good fatigue properties.

Acknowledgements We thank for the financial support to the Romanian National Authority for Scientific Research (PN09-450101, contract No. 45N/1.03.2009).

References

1. Jiang AQ, Lin YY, Tang TA (2007) Appl Phys Lett 91:202906
2. Nakamura T, Nakao Y, Kamisawa A, Takasu H (1994) Appl Phys Lett 65(12):1522
3. Aoki K, Fukuda Y, Numata K, Nishimura A (1996) Jpn J Appl Phys 35:2210
4. Asano G, Morioka H, Funakubo H, Shibutami T, Oshima N (2003) Appl Phys Lett 83:5506
5. Maeder T, Muralt P, Sagalowicz L (1999) Thin Solid Films 345:300
6. Norga GJ, Wouters DJ (2000) Integr Ferroelectr 31:1205
7. Yi JH, Seveno R, Gundel HW (1999) Integr Ferroelectr 23:99
8. Bai GR, Tsu IF, Wang A, Foster CM, Murray CE, Dravid VP (1998) Appl Phys Lett 72:1572
9. Trupina L, Miclea C, Tanasoiu C, Amarande L, Miclea CT, Cioangher M (2007) J Optoelectron Adv Mater 9(5):1508
10. Miclea C, Tanasoiu C, Miclea CF, Amarande L, Gheorghiu A, Spanulescu I, Plavitu C, Miclea CT, Cioangher MC, Trupina L, Iuga A (2007) J Eur Ceram Soc 27(13–15):4055
11. Ting CC, Chen SY, Liu DM (2001) Thin Solid Films 402:290
12. Ryden WD, Lawson AW (1970) Phys Rev B 1(4):1494
13. Fox GR, Sun S, Takamatsu T (2000) Integr Ferroelectr 31:147
14. Lee MS, Park KS, Nam SD, Lee KM, Seo JS, Lee SW, Lee YT, An HG, Kim HJ, Cho SL, Son YH, Kim YD, Jung YJ, Heo JE, Park SO, Chung UI, Moon JT (2002) Jpn J Appl Phys 41:6709
15. Glen RF, Shan S, Tomohiro T, (2000) Integr Ferroelectr 31(1):47